Observations of Supergradient Winds in the Tropical Cyclone Boundary Layer

Shannon L. McElhinney and Michael M. Bell
University of Hawaii at Manoa

Background

Two TC spin-up mechanisms (Smith et al. 2009)

1. Balanced dynamics
   a. Radial convergence of absolute angular momentum above BL (conserved)
   b. Explains expansion of tangential wind field

2. Unbalanced dynamics
   a. Radial convergence of absolute angular momentum within BL (not conserved)
   b. Most important at small radii

Background

Recently proposed mechanism for SEF (Huang et al. 2012)

1. Broadening of tangential wind field above BL
2. Increase in BL inflow outside primary eyewall
3. Supergradient wind develops at top of BL

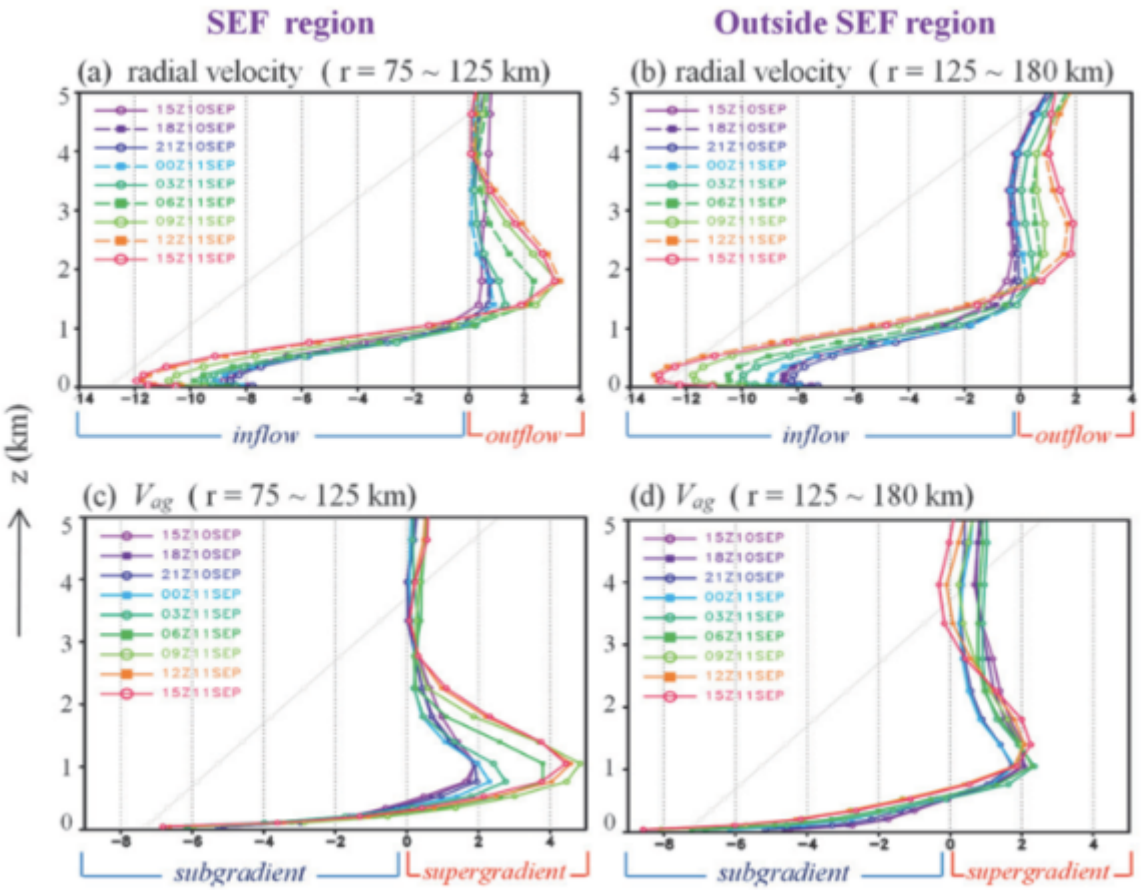

Figure from Huang et al. 2012

Background

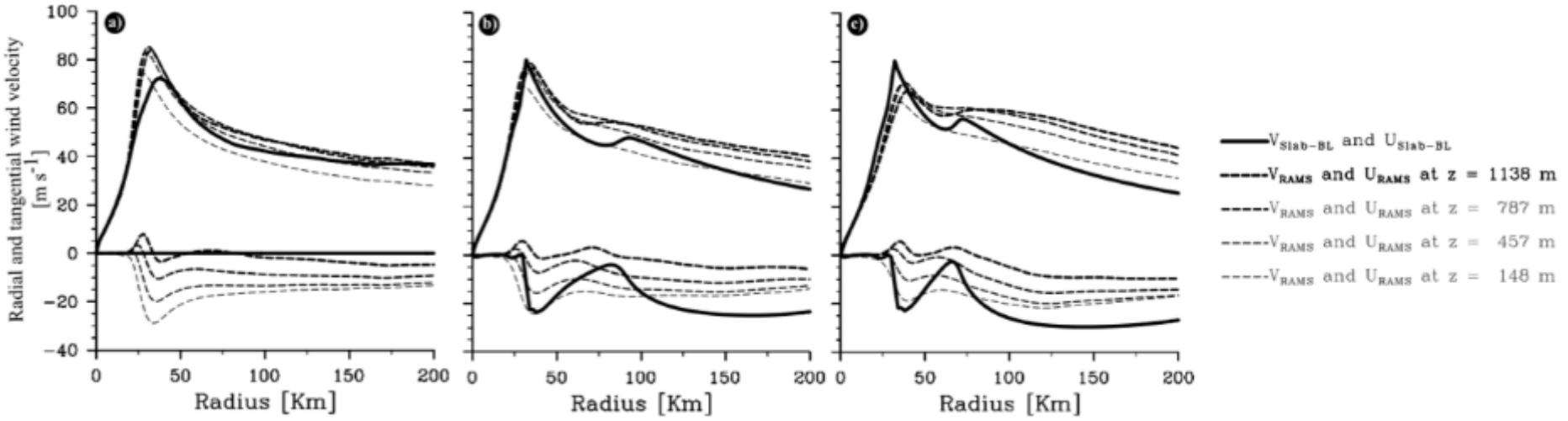

Unbalanced BL dynamics quantitatively important for contraction of secondary eyewall

Figure from Abarca and Montgomery 2013

Background

- The degree to which winds exceed gradient balance in observations is still unresolved.
- How well can observations quantify the magnitude of this jet?
- Operational models should include BL processes to improve prediction of SEF (Huang et al. 2012; Williams et al. 2013)

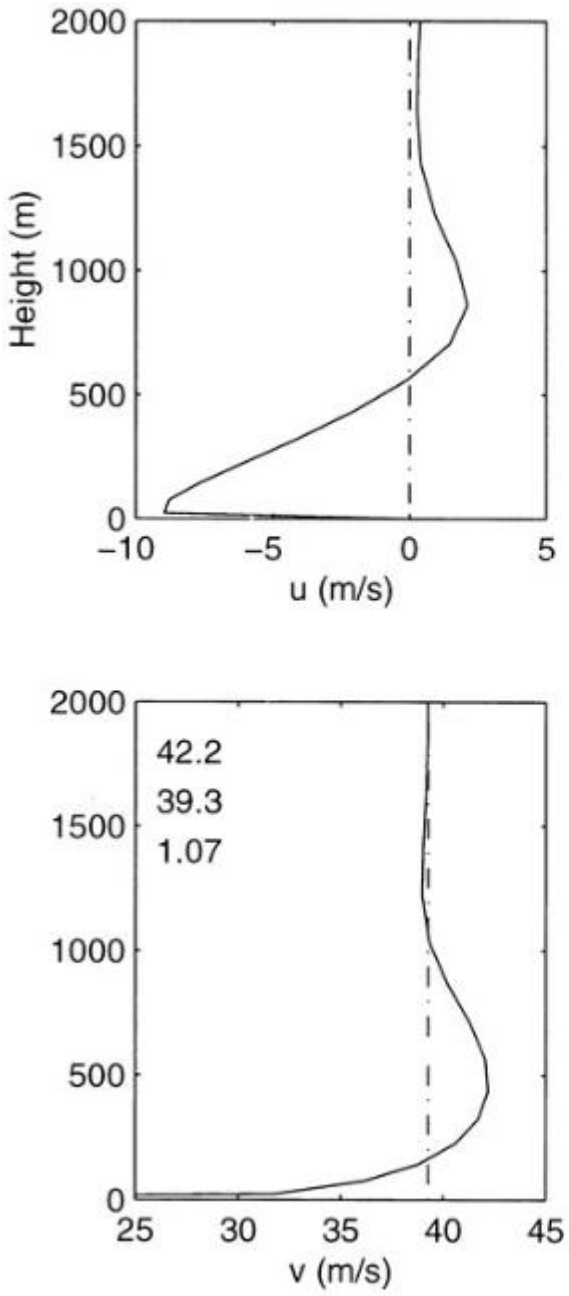

Figure from Kepert and Wang 2001

Methods

Methods

- Observations Used
  - Airborne Doppler radar
  - GPS Dropsondes
  - Flight level in situ
  - SFMR (in the future)

- Observation Limitations
  - Far from land
  - Extreme conditions
  - Sea clutter/sea spray
  - Attenuation
  - Large spatial extent

- SAMURAI (Spline Analysis at Mesoscale Utilizing Radar and Aircraft Instrumentation)
  - Spline-based 3-D variational analysis technique
  - Analysis in cylindrical coordinates
  - Outputs most likely TC fields

Methods: Case 1

- WRF Simulated Hurricane Rita (2005)
  - 84 hrs, quadruply nested to 666.7 m
  - Flew airborne Doppler radar through simulation

  (N-S straight line), 1.5 km height, point beam, no noise, flat surface
  - SAMURAI
  - Compared to model "truth" field

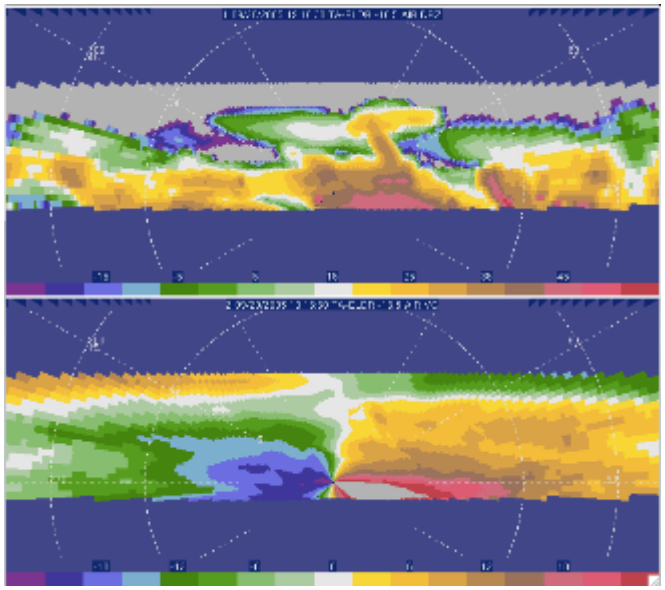

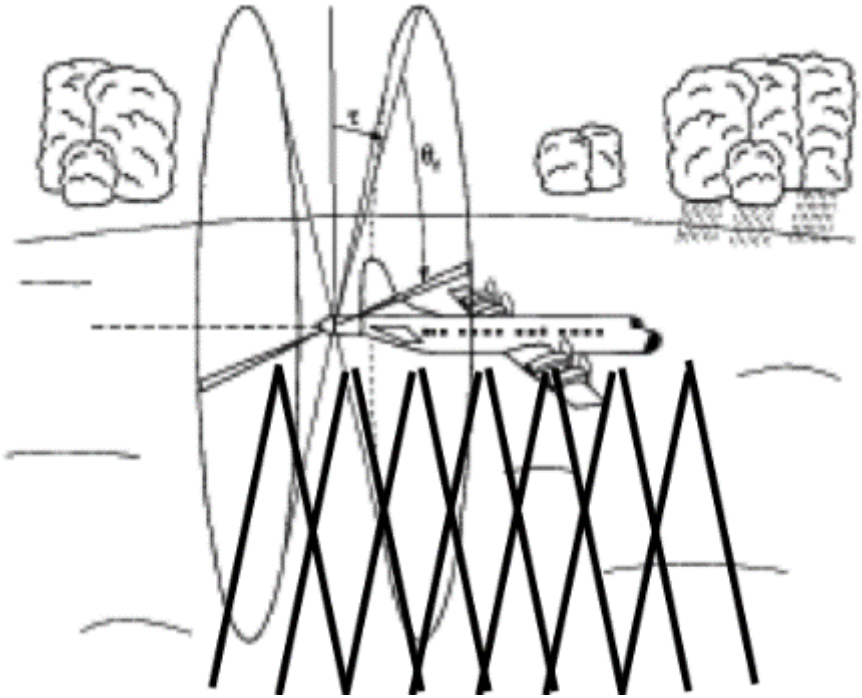

Methods: Case 2

- Real Hurricane Rita 9/22 18 UTC observations from RAINEX
  - Automated Radar QC in Soloii
  - SAMURAI
    - Test 1 (NOAA P3 radar)
    - Test 2 (NOAA P3 all observations)
    - Truth (ELDORA and NOAA P3 all observations)

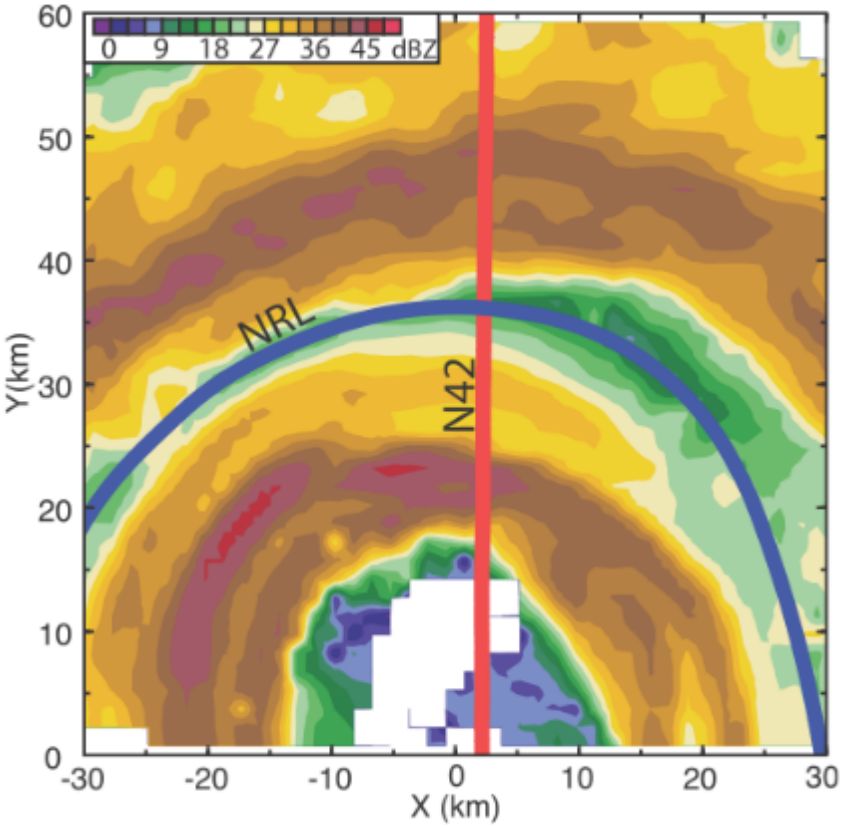

Figure from Bell et al., 2012b

Results

Case 1: Wind Analysis Results

Control run – only simulated radar observations put into SAMURAI

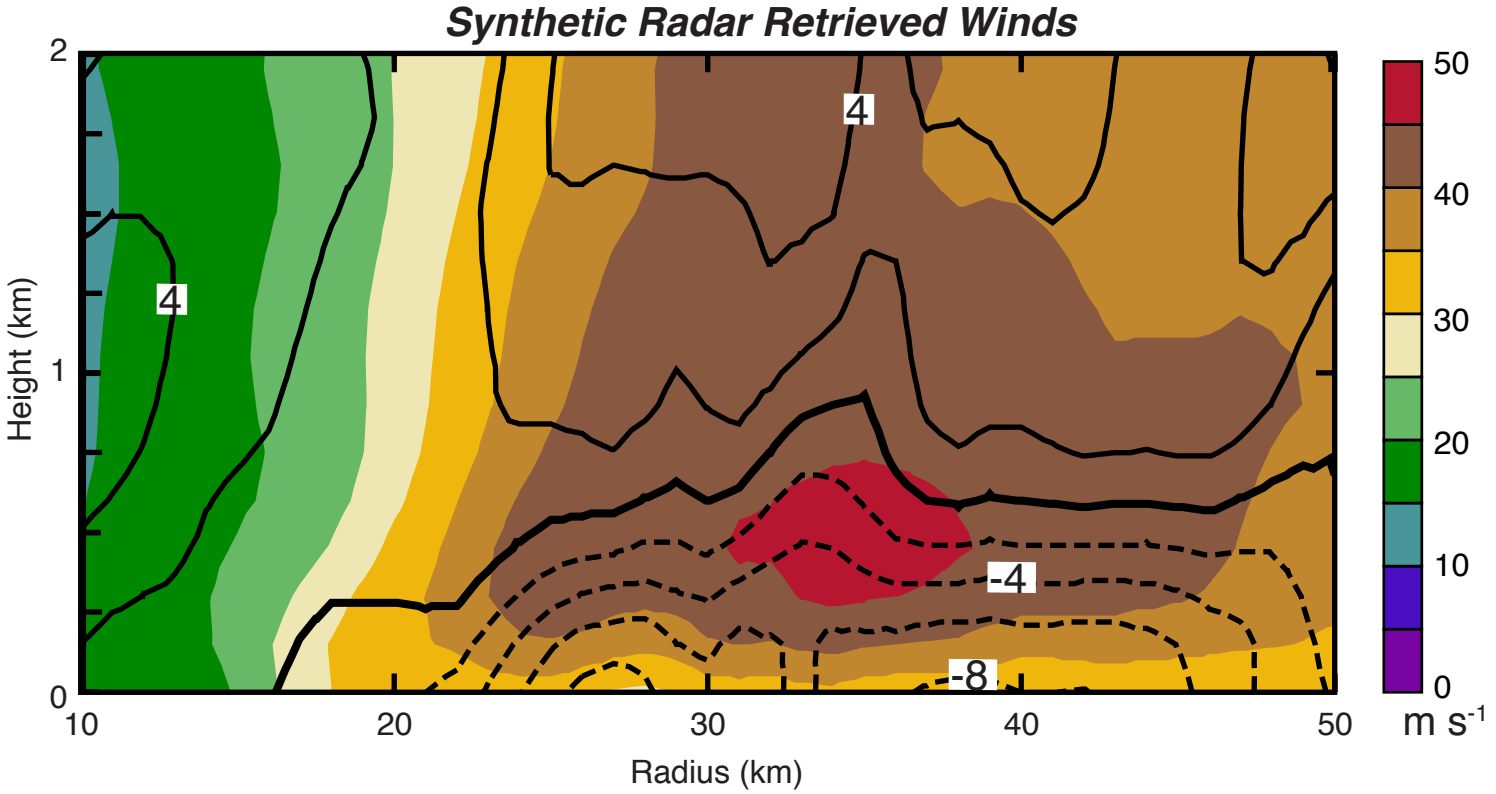

Case 1: Wind Analysis Results

Dtheta (degrees)					Radar	Dropsondes (km)					Flight-level	Error (m/s)	
5	10	15	20	25	Synthetic	1	2	4	6	8	1.5 km	RMSE V	RMSE U
				x	x							2.72	1.46
			x		x							4.31	1.74
		x			x							8.14	2.31
	x				x							12.37	3.37
x					x							18.42	5.48
				x	x	x						2.41	0.96
				x	x		x					2.36	0.86
				x	x			x				2.34	0.93
				x	x				x			2.34	1.03
				x	x					x		2.40	1.10
				x	x						x	2.35	1.39
				x	x	x					x	2.31	0.93

- Dropsondes can provide valuable information to help constrain the under-resolved along- track radar-derived winds (Hildebrand et al. 1996)
- No significant differences were found for the dropsonde data at different spatial resolutions – this should be different for thermodynamic retrieval

Case 1: Simulated Airborne Radar Observations

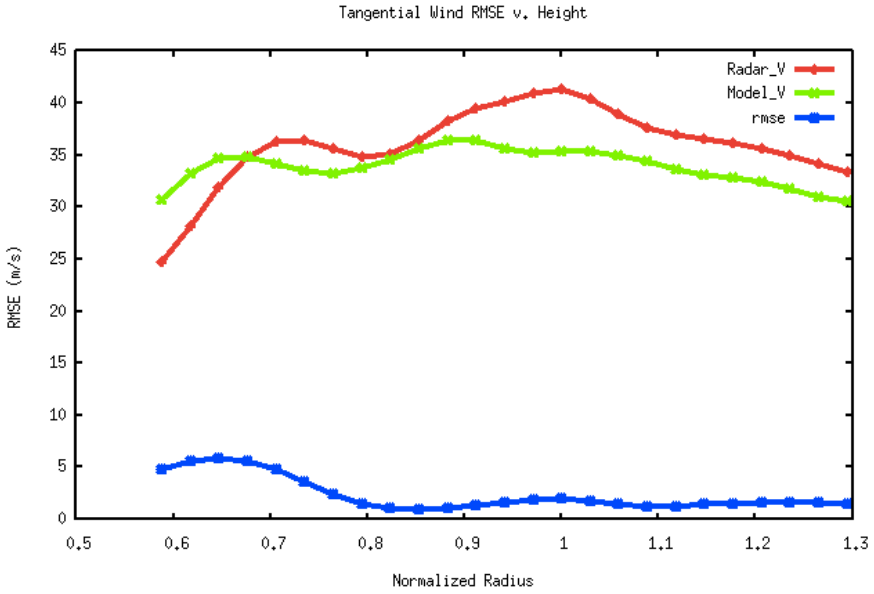

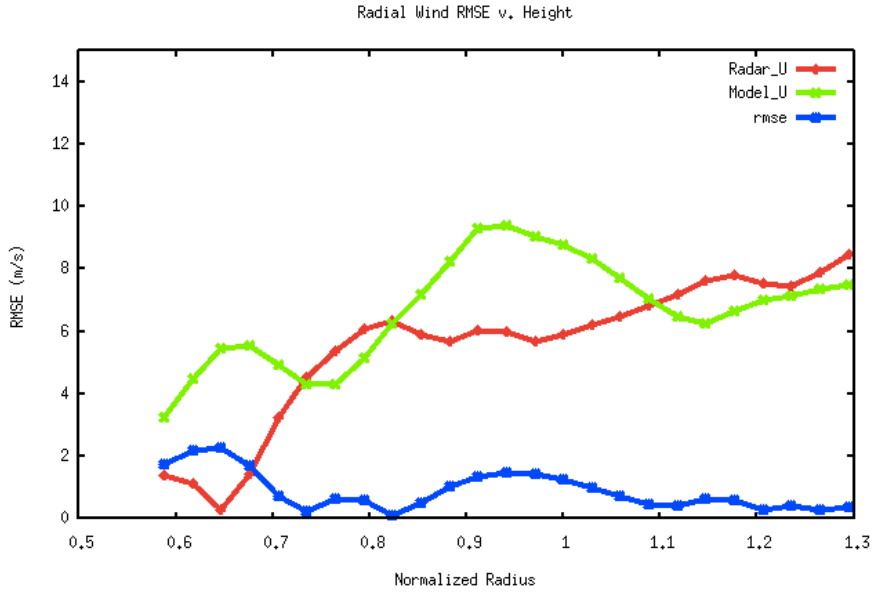

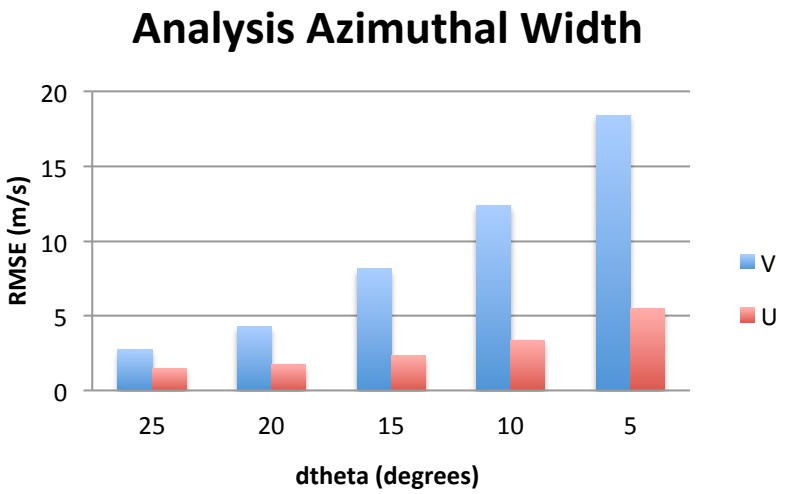

- Error in tangential wind (V) increases as analysis slice narrows
- Error in radial wind (U) increases, but not as much

- Red = control test wind
- Green = truth wind
- Blue = depth-averaged rmse

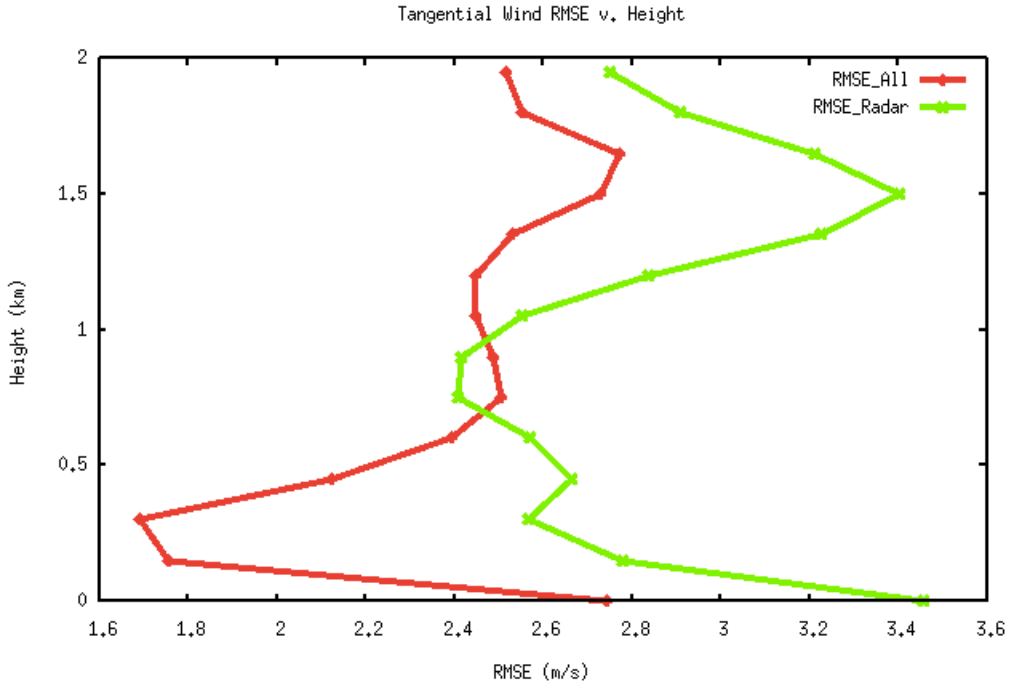
Tangential Wind RMSE v. Height
RMSE_All
RMSE_Radar
Height (km)
RMSE (m/s)
0
0.5
1
1.5
2
1.6
1.8
2
2.2
2.4
2.6
2.8
3
3.2
3.4
3.6

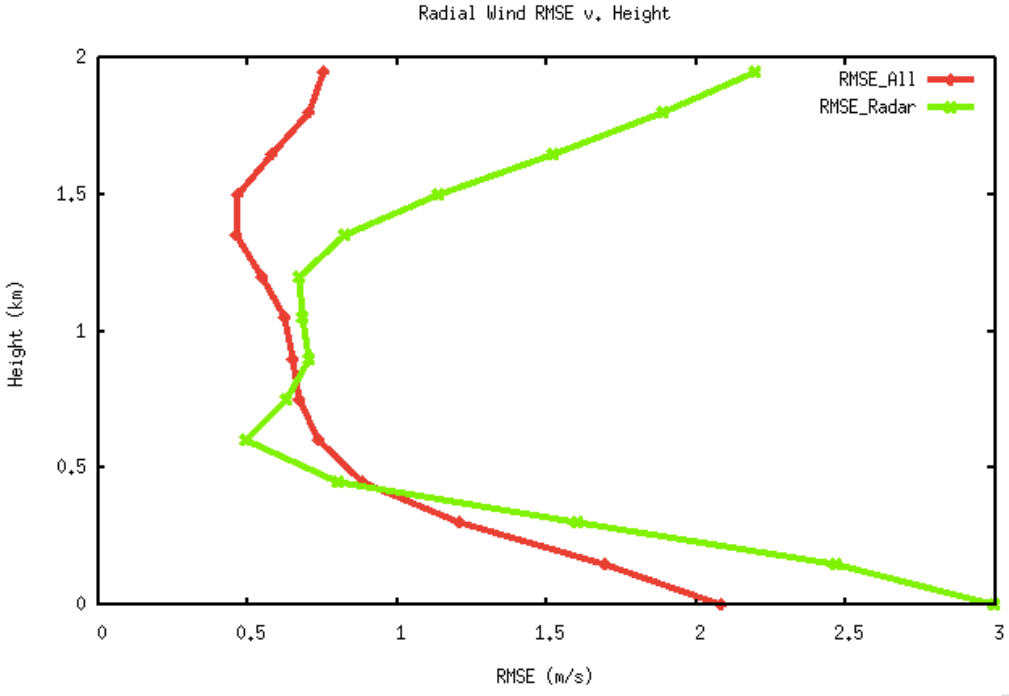
Radial Wind RMSE v. Height
RMSE_All
RMSE_Radar
Height (km)
RMSE (m/s)
0
0.5
1
1.5
2
0
0.5
1
1.5
2
2.5
3

Case 2: Wind Analysis Results

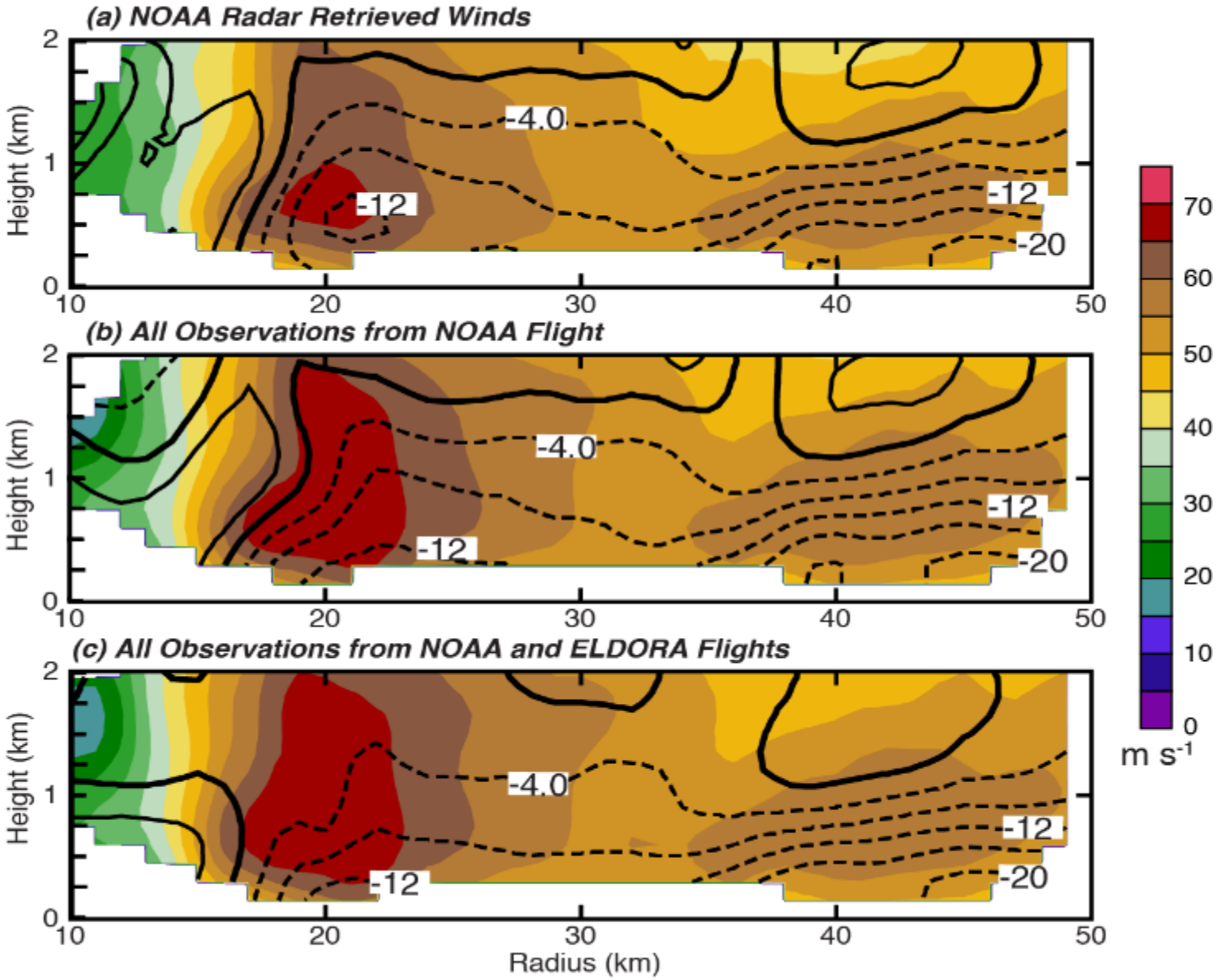

Case 2: Pressure Gradient

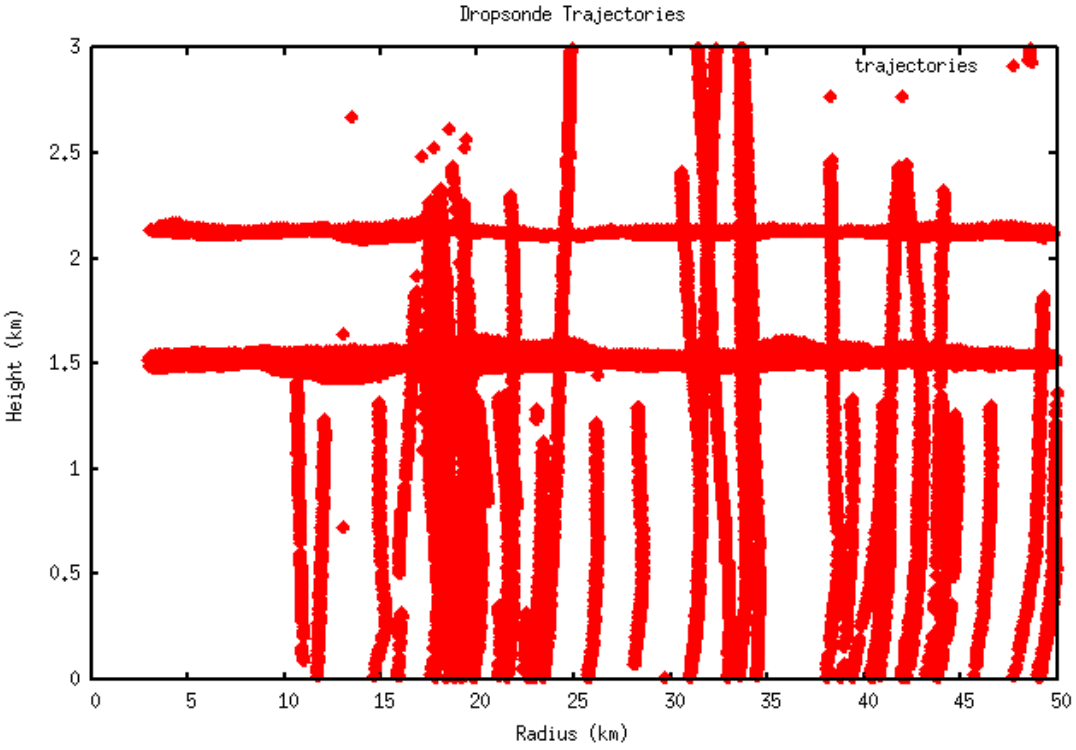

- Pressure Gradient was retrieved from dropsondes and flight level in situ
- Azimuthal average
- High sensitivity to data gaps

Case 2: Supergradient Wind

31 km

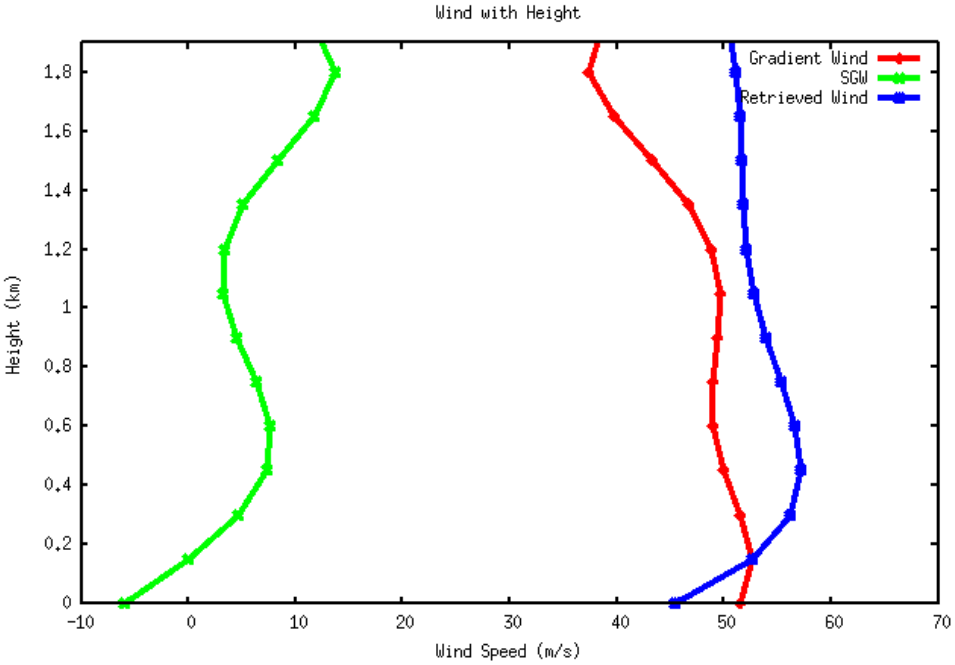

39 km

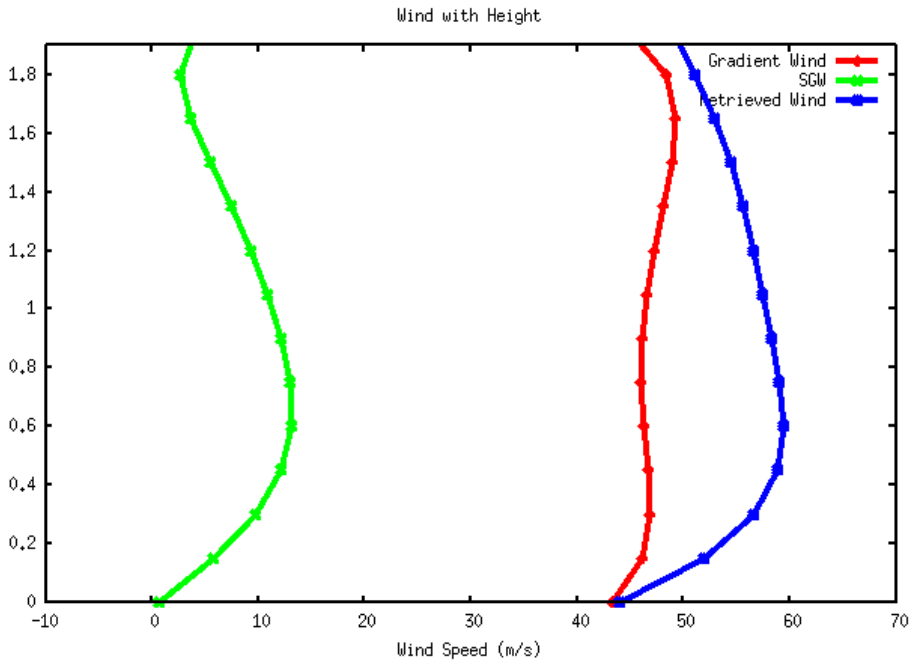

Limitations

- SAMURAI:
  - Unconstrained in data sparse regions but using a high filter eliminates small-scale detail
  - Recursive filter length scale: 6 km (radial), 300 m (vertical)

- Rita Observations:
  - Radar only retrieves wind where there is precipitation
  - Dropsonde distribution

Conclusions

- This technique can produce reasonable results with radar-derived winds alone, but incorporating multiple in situ measurements adds significant value
  - Mean wind errors of 1 - 2 m/s
  - 6 % for V and 26% for U

- Preliminary Findings with Synthetic Dataset:
  - Analysis azimuthal width results suggests a trade-off between azimuthal spatial resolution and wind accuracy
  - Flight-level data adds value to tangential (V) and radial (U) winds
  - Dropsondes add additional value
  - V errors are reasonable below 300 m, U down to 500 m

Conclusions

- Initial results show wind may be supergradient in Rita's secondary eyewall
  - Must complete pressure gradient error analysis
  - Additional uncertainty analysis using aircraft legs in different storm quadrants and at different times will help to improve error statistics

References

Abarca, Sergio F., and Michael T. Montgomery. "Essential Dynamics of Secondary Eyewall Formation." *Journal of the Atmospheric Sciences* 2013 (2013).

Bell, M. M., M. T. Montgomery, K. A. Emanuel, 2012: Air–Sea Enthalpy and Momentum Exchange at Major Hurricane Wind Speeds Observed during CBLAST. *J. Atmos. Sci.*, 69, 3197–3222.

Bell, M. M., M. T. Montgomery, W.-C. Lee, 2012: An Axisymmetric View of Concentric Eyewall Evolution in Hurricane Rita (2005). *J. Atmos. Sci.*, 69, 2414–2432.

Huang, Yi-Hsuan, Michael T. Montgomery, and Chun-Chieh Wu. "Concentric eyewall formation in Typhoon Sinlaku (2008). Part II: Axisymmetric dynamical processes." *Journal of the Atmospheric Sciences* 69.2 (2012): 662-674.

Kepert, Jeff, Yuqing Wang (2001). The Dynamics of Boundary Layer Jets within the Tropical Cyclone Core. Part II: Nonlinear Enhancement. *J. Atmos. Sci.*, 58, 2485–2501.

Lorsolo, S., J. A. Zhang, F. D. Marks, and J. Gamache, 2010: Estimation and mapping of hurricane turbulent energy using airborne Doppler measurements. *Mon. Wea. Rev.*, 138, 3656–3670.

Smith, Roger K., Michael T. Montgomery, and Nguyen Van Sang. "Tropical cyclone spin-up revisited." *Quarterly Journal of the Royal Meteorological Society* 135.642 (2009):1321-1335.

Williams, Gabriel J., et al. "Shock-like structures in the tropical cyclone boundary layer." *Journal of Advances in Modeling Earth Systems* (2013).

SAMURAI: Appendix B

- Uses an incremental form of the variational cost function that avoids the inversion of the background error covariance matrix by using a control variable $x\hat{}$, similar to the forms in Barker et al. (2004, Eq. 2) and Gao et al. (2004, Eq. 7):

$$J(x\hat{}) = 1x\hat{}^T x\hat{} + 1(HCx\hat{} - d)^T R{-}1(HCx\hat{} - d)$$

- The cost function is minimized using a conjugate gradient algorithm (Polak 1971; Press et al. 2002) to find the atmospheric state where the gradient with respect to $x\hat{}$ is:

$$\nabla J(x\hat{}) = (I + C^T H^T R{-}1HC)x\hat{} - C^T H^T R{-}1d$$

- A large background error standard deviation has the detrimental side effect of making the spline analysis unconstrained in data-poor regions
- The mean tropical sounding from Jordan (1958) was used as the reference state

Bell et al. 2012 (II)

BL Definition

- From Smith et al. (2009)
- Shallow layer of strong inflow near the surface
  - 500 – 1000m thick
  - Caused by friction with the sea surface

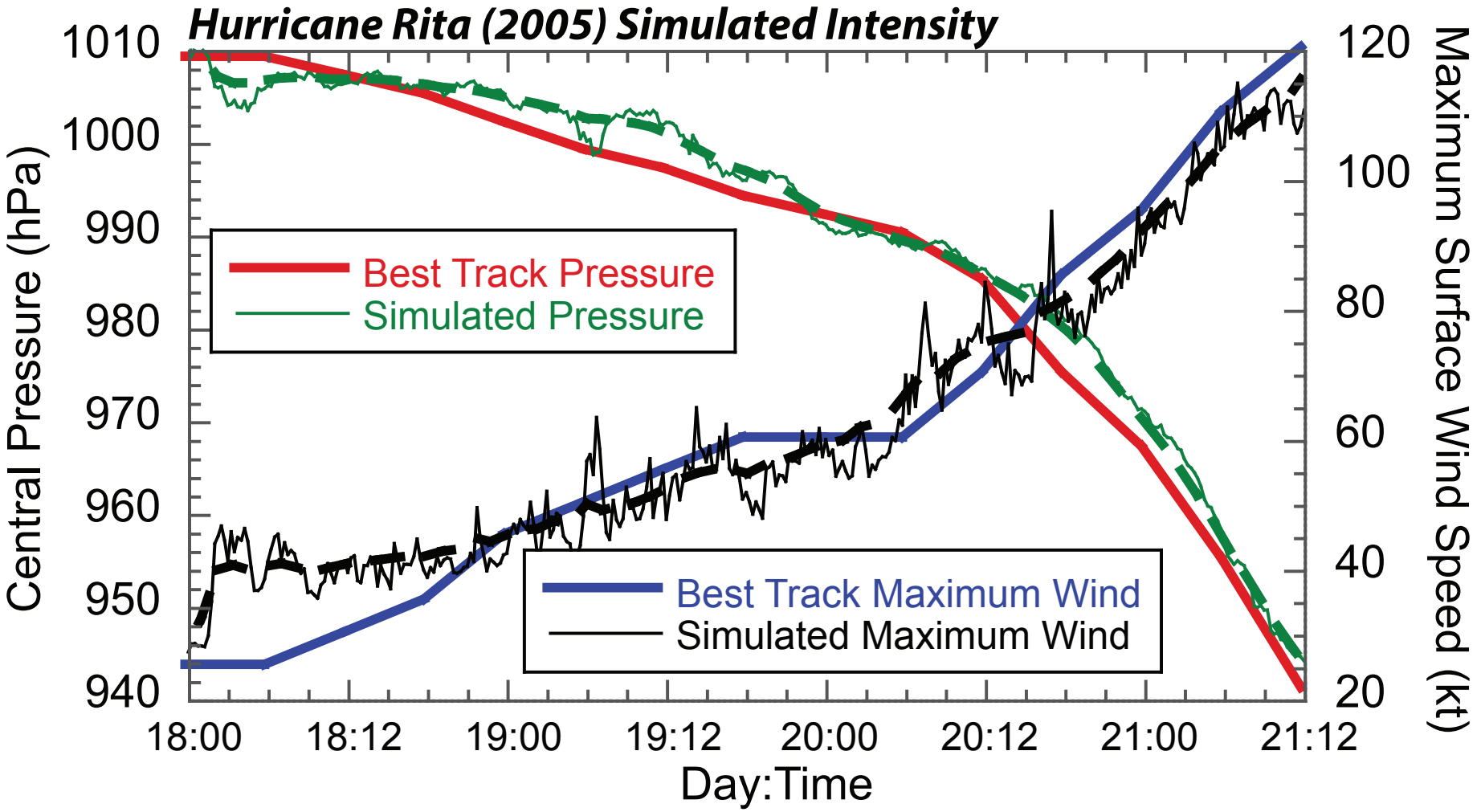
Hurricane Rita (2005) Simulated Intensity
Central Pressure (hPa)
Maximum Surface Wind Speed (kt)
Day:Time
1010
1000
990
980
970
960
950
940
120
100
80
60
40
20
18:00
18:12
19:00
19:12
20:00
20:12
21:00
21:12
Best Track Pressure
Simulated Pressure
Best Track Maximum Wind
Simulated Maximum Wind

Observations from GPS Dropsondes in Hurricane Mitch 1998

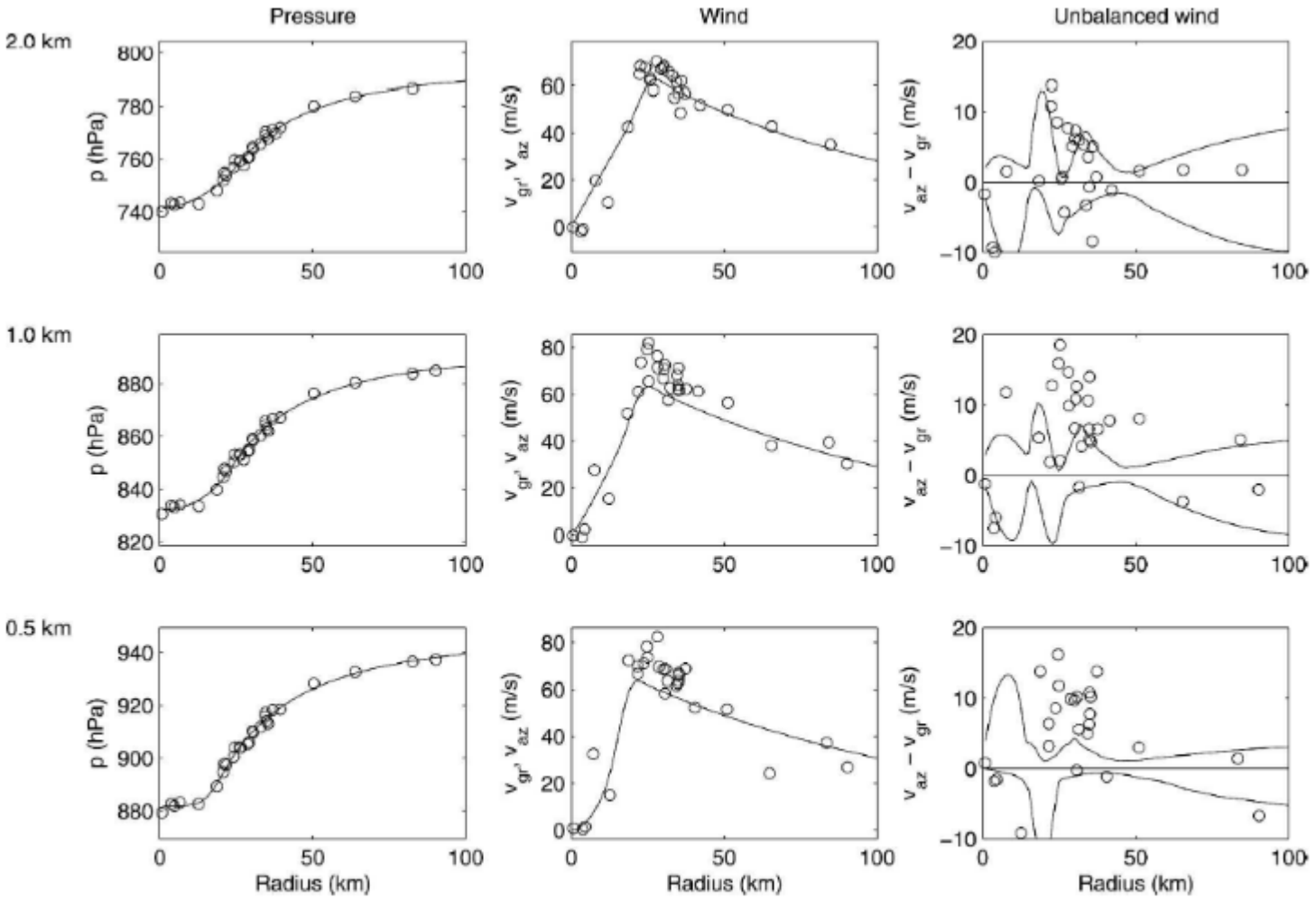

(Kepert, 2006)